Full Paper

Wiley Online Library

ELECTROANALYSIS

DOI: 10.1002/elan.202060323

Easily Multiplexable Immunoplatform to Assist Heart Failure Diagnosis through Amperometric Determination of Galectin-3

Sofía V. Piguillem[+],[a, b] Maria Gamella[+],[a] Pablo García de Frutos,[c] Montserrat Batlle,[d] Paloma Yáñez-Sedeño,[a] Germán A. Messina,[b] Martín A. Fernández-Baldo,[b] Susana Campuzano,*[a] María Pedrero,*[a] and José M. Pingarrón[a]

Abstract: This work reports the first electrochemical immunoassay involving magnetic microbeads (MBs) for the determination of galectin-3 (Gal-3), a β-galactosidase-binding lectin that acts as mediator of heart failure (HF). MBs-captured sandwich-type immune complexes and amperometric detection at disposable screen-printed carbon electrodes were used. The immunoplatform showed a detection limit of 8.3 pg mL^{-1}, good reproducibility, and excellent selectivity. The endogenous concentration of Gal-3 in human plasma from HF patients was determined with results in agreement with those obtained using ELISA. The multiplexing feasibility of the developed immunoplatform was demonstrated for the simultaneous determination of Gal-3 and N-terminal pro-brain natriuretic peptide (NT-proBNP).

Keywords: Electrochemical immunoplatform · Magnetic beads · Galectin-3 · Plasma samples · Heart failure

1 Introduction

With the aging of population and increase of cardiovascular health risk factors, the prevalence rate of heart failure (HF) continues rising, becoming a serious challenge to the public health. Therefore, a rapid and accurate diagnosis is essential to improve HF patients' outcomes. However, HF is not easy to diagnose since clinical symptoms are often non-specific [1]. HF diagnosis is usually based on the combination of various parameters such as patient's history, physical examination and laboratory tests or imaging techniques, which require well-trained operators and expensive equipment, sometimes not accessible in the majority of primary healthcare facilities. Accordingly, objective evaluation within clinically actionable times and preferably in a minimally invasive manner using specific biomarkers may be one avenue for routinely evaluation in order to diagnose HF, assess the risk of future events, and guide efficient therapy [2,3].

Brain natriuretic peptide (BNP) and N-terminal pro-brain natriuretic peptide (NT-proBNP) are biomarkers of great value in the diagnosis, prognosis evaluation and clinical management of HF. However, they are influenced by multiple factors such as age, renal function, or body-mass index resulting in a large natural variation amongst patients [1,4]. In consequence, seeking for complementary biomarkers able to provide additional information to improve risk stratification and to individualize therapy [5] is highly desirable. In this context, several human clinical studies have studied the role of the lectin galectin-3 (Gal-3) in the development of HF [6]. Gal-3 is a 30 kDa member of the carbohydrate-binding protein family of lectins and plays an important regulatory role in cardiac fibrosis and increased expression of collagens, which are key factors in the development of heart hypertrophy and progression of HF [7,8]. Interestingly, as Gal-3 is expressed before the development of overt clinical HF [9], blood circulating levels of Gal-3 are proposed as prognostic for acute HF in patients providing additive information to natriuretic peptide levels [10]. It has been shown that

[a] S. V. Piguillem,[+] M. Gamella,[+] P. Yáñez-Sedeño, S. Campuzano, M. Pedrero, J. M. Pingarrón
Analytical Chemistry Dept., Faculty of Chemistry, Complutense University of Madrid. E-28040 Madrid, Spain
E-mail: susanacr@ucm.es
mpedrero@quim.ucm.es

[b] S. V. Piguillem,[+] G. A. Messina, M. A. Fernández-Baldo
INQUISAL, Departamento de Química. Universidad Nacional de San Luis, CONICET. Chacabuco 917. D5700BWS. San Luis, Argentina

[c] P. García de Frutos
Department of Cell Death and Proliferation IIBB-CSIC, and IDIBAPS, Barcelona, Spain

[d] M. Batlle
Institute of Biomedical Research August Pi i Sunyer (IDIBAPS) and The Cardiovascular Clinic Institute, Hospital Clínic de Barcelona, Spain

[+] These authors have contributed equally to this work

Supporting information for this article is available on the WWW under https://doi.org/10.1002/elan.202060323

activated macrophages release Gal-3, whose increased levels are related to poor prognosis in HF [8], even suggesting that serum Gal-3 is not only elevated in patients with stable HF, but may also be predictive of adverse outcomes in Acute HF Syndromes [10].

Several methods for Gal-3 determination have been used. They include western blot and enzyme-linked immunosorbent assays (ELISAs) [11–15], immunohistochemistry [16–18], immunoassays [19,20], mass spectrometry [21], flow cytometry [22], reverse transcription polymerase chain reaction (RT-PCR) [23,24], surface plasmon resonance [25,26], and the "routine Gal-3" assay (Abbott Diagnostics) [20,27]. Even though these methods present high sensitivity and selectivity, they must be improved since they are time-consuming and depend on sophisticated, expensive, and centralized equipment, also needing skilful operators. Therefore, sensitive, simple, rapid, and low-cost methods for Gal-3 determination even at decentralized settings are highly desirable.

In this context, electrochemical immunosensors have attracted the attention of many scientists in recent years. Their features such as high sensitivity, ease of operation and low manufacturing cost, as well as the possibility of simultaneous multi-target analysis, and miniaturization make them very interesting devices for the analysis of clinical biomarkers [28,29]. Among the wide number of strategies used in the development of electrochemical immunosensors, that involves magnetic microparticles (MBs) shows unique and attractive physicochemical properties that make them handy in a wide range of applications [30]. Their integration into electrochemical immunosensing devices enhances sensitivity through efficient capturing and pre-concentration of the target analyte and allows easy washing and isolation in the presence of external magnetic fields thus aiding to remove sample matrix effects [31]. So far, there is only one electrochemical immunosensor reported for the determination of Gal-3, involving an integrated format [32]. Although this immunosensor exhibits an excellent sensitivity (allowing detection of as little as 33.33 $fg\,mL^{-1}$ Gal-3 in spiked serum samples) it requires time-consuming and multi-step preparation of nanocomposites of N-doped graphene nanoribbons immobilized Fe-based-Metal-organic frameworks deposited with Au nanoparticles (N-GNRs–Fe-MOFs@AuNP) and of AuPt-Methylene blue (AuPt–MB) as electrode modifiers and labels, and to immobilize capture and detection antibody, respectively. The immunoplatform required more than 12 h for its preparation, apart from the 18 and 6 h, demanded by the synthesis of N-GNRs–Fe-MOFs@AuNP and AuPt–MB, respectively.

Hence, the purpose of this article is to report the first electrochemical sandwich-type bioassay for the determination of Gal-3 based on the use of MBs and disposable electrodes. Through the immobilization of the capture antibody on HOOC–MBs and the modified MBs incubation in a mixture solution that contains the analyte and a specific biotinylated detector antibody labelled with a streptavidin-horseradish peroxidase (Strep-HRP) polymer. The amperometric detection of the affinity reactions was performed using disposable screen-printed carbon electrodes (SPCEs) and the hydroquinone (HQ)/H_2O_2 system. The immunosensor achieves a good sensitivity and selectivity and was successfully applied to the analysis of Gal-3 in human plasma samples from patients followed for HF. In addition, since there is limited specificity of using a single cardiac biomarker to diagnose heart problems and Gal-3 is thought to provide independent and additive information to natriuretic peptides testing, we also report the use of an electrochemical immunoplatform for the simultaneous determination of Gal-3 and NT-proBNP.

2 Experimental

A description of apparatus, electrodes, reagents, and solutions can be found in the Supporting Information.

2.1 Preparation of the MBs-based Sandwich Immunocomplexes

2.1.1 MBs Bearing the Gal-3 Sandwich Immunocomplexes

A 3 µL-aliquot of the homogenized commercial HOOC–MBs suspension was transferred into a 1.5-mL micro-centrifuge tube and washed twice with 50 µL MES buffer for 10 min (25 °C, 950 rpm). The MBs were then magnetically separated by placing them in a magnetic separator for 3 min in order to remove the supernatant after all the involved steps. Thereafter, the activation of the MBs surface carboxylic groups was carried out by using 25 µL of a freshly prepared EDC/sulfo-NHS solution for 35 min (25 °C, 950 rpm). After washing the activated MBs twice with MES buffer, a 30 min incubation step (25 °C, 950 rpm) in 25 µL of a 10 $\mu g\,mL^{-1}$ CAb solution prepared in MES buffer was performed, washing the CAb-MBs conjugates twice with MES buffer solution. Subsequently, the residual activated groups were blocked by incubating the modified CAb-MBs in a 1.0 M ethanolamine solution for 1 h (25 °C, 950 rpm). Finally, the CAb-MBs were washed once with 0.1 M Tris-HCl buffer (pH 7.2), twice with PBS, and stored at 4 °C in sterilized PBS until their use.

The Gal-3 sandwich immunocomplexes were formed by incubating the CAb-MBs in 25 µL of a mixture solution that contained Gal-3 standard (or the sample to analyze) and 0.5 $\mu g\,mL^{-1}$ B-DAb for 30 min (25 °C, 950 rpm) prepared in casein blocking buffer solution. After washing twice, the B-DAb-Gal-3-CAb-MBs were incubated in a 1/5,000 diluted Strep-HRP solution (prepared in casein blocking buffer) for 30 min (25 °C, 950 rpm). Finally, the sandwich-MBs immunocomplexes were washed twice and re-suspended in 50 or 5 µL of 0.05 M phosphate buffer, pH 6.0, to carry out the single or dual amperometric measurements, respectively.

2.1.2 MBs Bearing the NT-proBNP Sandwich Immunocomplexes

A similar protocol was followed for the preparation of MBs bearing the NT-proBNP sandwich immunocomplexes. The activated HOOC-MBs were incubated for 30 min (25 °C, 950 rpm) with 25 µL of 25 µg mL^{-1} NT-proBNP CAb made in MES buffer and washed twice with 50 µL of MES buffer. The CAbs-MBs were then incubated for 60 min (25 °C, 950 rpm) in a 1.0 M ethanolamine solution made in 0.1 M phosphate buffer, pH 8.0, followed by one washing step with 50 µL of 0.1 M Tris-HCl buffer, pH 7.2, and twice with 50 µL of 0.01 M PBS solution, pH 7.5. The resulting MBs were stored at 4 °C in sterilized PBS until their use.

The prepared CAb-MBs were subsequently incubated in 25 µL of a mixture solution that contained NT-proBNP standards (or the sample to be analyzed), 0.5 µg mL^{-1} B-DAb and a 1/1,000 dilution Strep-HRP made in commercial blocker casein solution for 30 min at 25 °C, 950 rpm. Finally, the modified MBs were rinsed twice with 50 µL of commercial blocker casein solution and kept in 5 µL of 0.05 M phosphate buffer, pH 6.0, to carry out the dual amperometric measurements.

2.2 Amperometric Measurements

Once the whole suspension of MBs modified with the sandwich immunocomplexes were drop casted on the WE surface of the SPCE previously introduced in the appropriate magnet containing-PMMA casing, the SPE/casing ensemble was connected to the potentiostat through the specific cable connector and placed into an electrochemical cell that contained 10 mL of 0.05 M phosphate buffer solution (pH 6.0) and 1.0 mM fresh HQ. A detection potential value of −0.2 V (*vs* the Ag pseudoreference electrode) was selected for the single or dual amperometric measurements [33] upon addition of 50 µL of a 0.1 M freshly prepared H_2O_2 solution. The recorded amperometric signals were calculated as the difference between the steady state and the background currents, being the given values the mean value of three replicates. Error bars were estimated as triple of the standard deviation of each set of replicas (confidence intervals calculated for $\alpha = 0.05$).

2.3 Analysis of Plasma Samples

The developed amperometric immunoassay was applied to the analysis of human plasma samples provided by Hospital Clinic of Barcelona from healthy individuals and patients which are being followed for heart damage after obtaining written informed consent from all of them. The plasma samples, stored at −80 °C, were analyzed after a 10-times dilution with blocking buffer solution. The endogenous concentrations of Gal-3 were determined by using the standard additions method by spiking the diluted plasma samples with increasing Gal-3 concentrations (500–1,000 pg mL^{-1}).

The results obtained with the immunoplatforms were compared with those provided by the ELISA method using the same immunoreagents and the protocol described by Muñoz et al. [34], using the following reagent concentrations: 50 µL of 4.0 µg mL^{-1} CAb solution (prepared in PBS) 50 µL of Gal-3 standard solutions or diluted plasma sample, (made in Reagent Diluent solution), 50 µL of 25 ng mL^{-1} B-DAb solution (in Reagent Diluent solution) and 1/5,000 Strep-HRP-diluted in Reagent Diluent solution. The determination of Gal-3 in plasma samples was performed by interpolating the optical density obtained for the 10-times diluted samples into the calibration plot constructed with standards in the 250–2,000 pg mL^{-1} range.

3 Results and Discussion

3.1 Immunoplatform for the Determination of Gal-3

Figure 1 illustrates schematically the different steps involved in the preparation and performance of the immunosensor developed for the determination of Gal-3. Covalent immobilization of CAb on the surface carboxylic groups of MBs was performed through EDC/sulfo-NHS chemistry. Once the remaining activated surface sites were blocked with ethanolamine, the target Gal-3 was sandwiched with a B-DAb further labeled with Strep-HRP polymer. The MBs bearing the sandwich immunoconjugates were magnetically captured on the WE surface of the SPCEs and the cathodic current variation was recorded at −0.2 V *vs* the Ag pseudoreference electrode using the H_2O_2/HQ system. This well-known and widely used detection mechanism in amperometric biosensing [35] involves the enzymatic reduction of H_2O_2 by HRP and the regeneration of the oxidized HRP by HQ. The oxidized form of the mediator, benzoquinone (BQ), is reduced at the applied constant potential on the electrode surface, providing a cathodic current proportional to the concentration of the target protein in the sample.

3.1.1 Optimization of Working Variables

The influence of the experimental conditions on the immunosensing amperometric signal was evaluated. The tested working variables, the assessed ranges as well as the chosen values, are listed in Table 1 and the results shown in Figure 2. The optimal values were selected according to the ratio obtained between the amperometric signals measured at −0.2 V (vs. the Ag pseudoreference electrode) for 0.0 (blank, B) and 1.0 ng mL^{-1} Gal-3 standard (signal, S) (signal-to-blank, S/B ratio).

Figures 2a and 2b show the effect of the CAb concentration and incubation time, respectively. The S/B ratio increased with the CAb concentration up to 10 µg mL^{-1} and levelled off for larger CAb concentrations, probably due to the increase in the non-specific binding

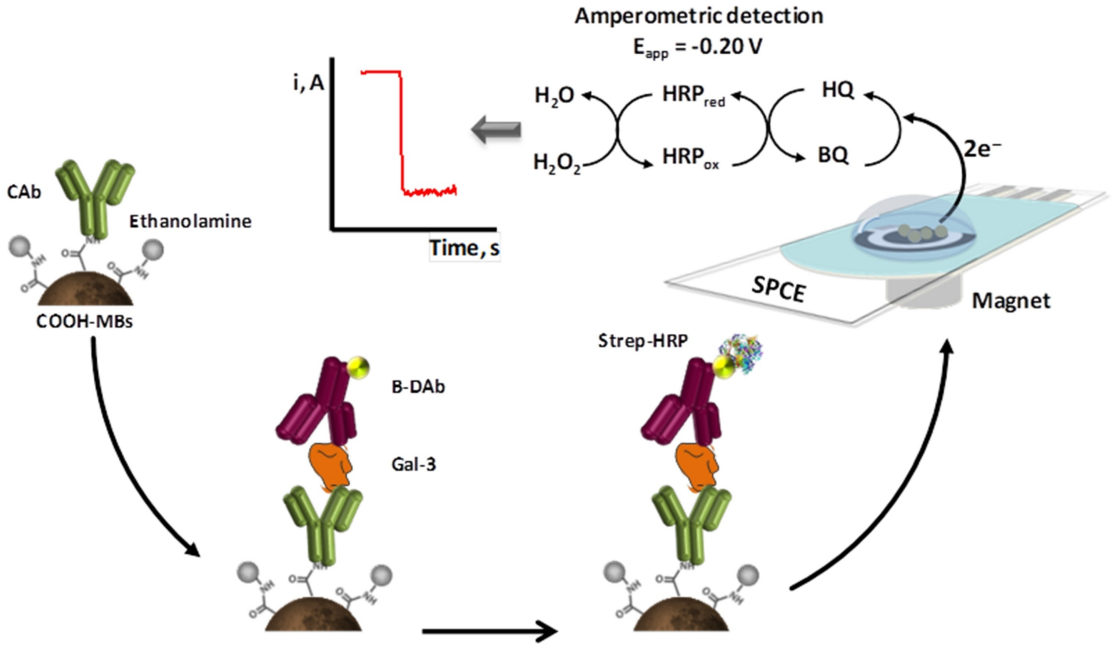

Fig. 1. Schematic display of the preparation and functioning of the MBs-based immunoassay for the amperometric determination of Gal-3.

Table 1. Experimental variables evaluated for the amperometric determination of Gal-3 using the developed magnetoimmunoplatform.

Variable	Tested range	Selected value
CAb concentration, μg mL^{-1}	0.0–50.0	10.0
Incubation time with CAb, min	0–60	30
Number of assay steps	1–3	2
B-DAb concentration, μg mL^{-1}	0.25–2.5	0.5
Incubation time with Gal-3 + B-DAb mixture, min	15–60	30
Strep-HRP dilution	1/50,000–1/500	1/5,000
Incubation time with Strep-HRP solution, min	15–60	30

between the CAb and the B-DAb in the absence of Gal-3. These results also show there was no discrimination for the presence of Gal-3 when the MBs were not modified with CAb, according to the rationale of the sandwich immunoassay strategy depicted in Figure 1. Hence, a CAb concentration of 10 μg mL^{-1} was chosen for further experiments. Regarding the CAb incubation time, (Figure 2b) 30 min was enough for efficient CAb attachment on the MBs.

Several working protocols involving a different number of 30-min incubation steps starting from the preparation of CAb-MBs were also tested (Figure 2c): 1) a single incubation step in a mixture solution containing Gal-3, B-DAb and Strep-HRP; 2a) two consecutive steps consisting of the incubation in: i) a mixture solution containing Gal-3 and B-DAb and ii) the Strep-HRP solution; 2b) two sequential incubation steps in: i) a Gal-3 solution and ii) a mixture solution containing B-DAb and Strep-HRP; and 3) three sequential steps in i) Gal-3, ii) B-DAb and iii) Strep-HRP solutions. Figure 2c shows that the best S/B ratio was obtained when the 2a) protocol was applied, which can be attributed to the decrease in the nonspecific binding between CAb and B-DAb when the B-DAb is at the same time as the target protein in homogeneous solution (see white 2a bar). This 2-step working protocol (protocol 2a), of acceptable complexity and test time, was selected for the immunoplatform development.

Figures 2d and 2e show as a better S/B ratio was achieved for a B-DAb concentration in the Gal-3 + B-DAb mixture solution of 0.5 μg mL^{-1} and for an incubation time of 30 min. Larger B-DAb concentrations provoked smaller S/B ratios due to a significant increase in non-specific B-DAb adsorptions in the absence of Gal-3 (Figure 2d). Moreover, larger incubation times of CAb-MBs in the mixture solution than 30 min provided similar S/B values since there was no significant difference between the amperometric signals obtained in the absence or in the presence of Gal-3 (Figure 2e).

Regarding the dilution and incubation time with the Strep-HRP solution, higher S/B ratios were achieved using a 1/5,000 dilution (Figure 2f) and a 30 min incubation time (Figure 2g). As it can be observed, a decrease in the S/B ratio was obtained when higher concentrations or incubation times were used as a result of the slight increase and decrease in the amperometric responses obtained in the absence and in the presence of Gal-3, respectively.

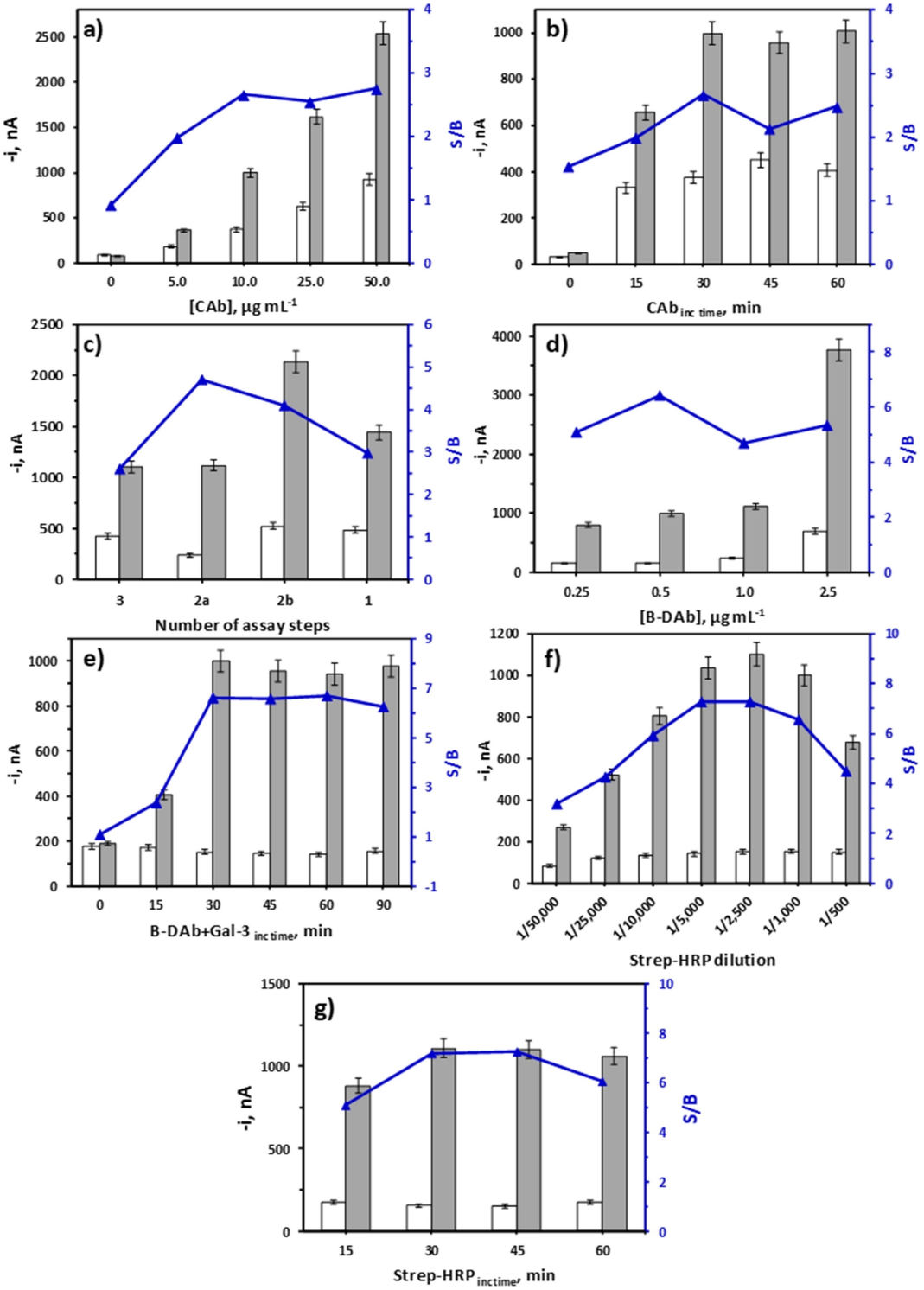

Fig. 2. Assessment of the influence of the: concentration (a) and incubation time of CAb (b); number of incubation steps (c); B-DAb concentration (d) and incubation time of CAb-MBs in the Gal-3 + B-DAb mixture solution (e); concentration (f) and incubation time of Strep-HRP loading (g), on the recorded amperometric signals in the absence (white bars) or in the presence (grey bars) of 1.0 ng mL^{-1} Gal-3 standards, and the obtained signal-to-blank ratios (S/B, blue triangles and lines). Error bars estimated as triple of the standard deviation (n = 3).

3.1.2 Analytical Characteristics

The amperometric determination of Gal-3 was carried out by constructing a calibration plot under the optimized working conditions that fitted into the equation: $-i\ (nA) = (818 \pm 28)$ [Gal-3] $(nA\,ng^{-1}\,mL) + (186 \pm 50)\ (nA)$ (Figure 3). The linear range ($r^2 = 0.998$) extended between 2.8×10^{-2} and 5 ng mL^{-1}. A LOD of 8.3 pg mL^{-1} was calculated following the $3 \times s_b/m$ criterion, where s_b was estimated as the standard deviation for 10 measurements recorded in the absence of Gal-3 and m is the slope of the linear calibration plot. Interestingly, these analytical features are suitable for the determination of Gal-3 considering its described range in clinical samples (1.4–94.8 ng mL^{-1}) [36,37]. It is worth remarking that reference values of 18 ng mL^{-1} (males) and 20 ng mL^{-1} (females) with values ranging between 5.0 and 24.4 ng mL^{-1} are reported in serum of cardiac healthy individuals [20], while reported values of Gal-3 in plasma samples range between 14 and 20 ng mL^{-1} [5,38,39]. Moreover, different studies have reported several cut-off values of Gal-3 of: 7.57 ng mL^{-1} in serum for predicting atrial fibrillation in patients with acute myocardial infarction [40], 10.8 ng mL^{-1} in plasma to discriminate HF patients [7], and 17.7 ng mL^{-1} in plasma to discriminate patients with acute and chronic HF (CHF) [36].

Regarding the reproducibility of the developed method, a relative standard deviation (RSD) value of 7.7 %, was obtained by measuring the responses given by 8 different MBs-based immunoplatforms prepared in the same manner (at a concentration level of 1.0 ng mL^{-1} of Gal-3), which indicates the great reproducibility of the developed methodology.

The long-term stability of prepared immunocaptors (CAb-MBs) was checked by keeping them at 4 °C in sterilized PBS (pH 7.5) solution. The control chart was built by using the calculated mean value of 10 amperometric measurements of a 1.0 ng mL^{-1} Gal-3 standard solution on the first day of the study (the day the CAb-MBs were prepared) as the central value, and $\pm 3 \times s$ of this value as the upper and lower control limits, respectively. Importantly, the amperometric signals obtained with the stored magnetic bioconjugates continued within the control limits for 60 days.

There are just few electrochemical biosensors for Gal-3 determination reported in the literature. To the best of our knowledge, there are only three papers for this purpose [32,41,42]. Two of them used Gal-3 ligand probes, galactose-containing single-walled carbon nanotubes [42], achieving a LOD of 0.156 μg mL^{-1}, and poly (amido amine) (PAMAM) dendrimers used as scaffold for lactose-ferrocene conjugates and gold nanoparticles [41] with a LOD of 160 nM (~ 4.8 μg mL^{-1}). Tang et al. proposed a sandwich-type electrochemical immunosensor for Gal-3 involving the use of a N-GNRs–Fe-MOFs@AuNPs-modified glassy carbon electrode (GCE) and AuPt–MB nanocomposites as signal amplification probes, reaching a LOD of 33.33 fg mL^{-1} [32]. This LOD is better than the achieved in this work (8.3 pg mL^{-1}). However, our method does involve neither the use of time-consuming multireagent/multistep processes for the preparation of the nanomaterials and the electrode surface modification nor the use of signal amplification tools. Importantly, the achieved sensitivity is clearly sufficient to tackle the determination in clinical samples where the mean values for healthy individuals (~ 17 ng mL^{-1}) are far above. In addition, the analysis time is shorter (60 min *vs* 120 min). All these characteristics make the developed immunosensor to meet better the requirements of bedside Gal-3 determination.

Furthermore, the determination of Gal-3 using surface plasmon resonance (SPR) based on lactose-modified gold

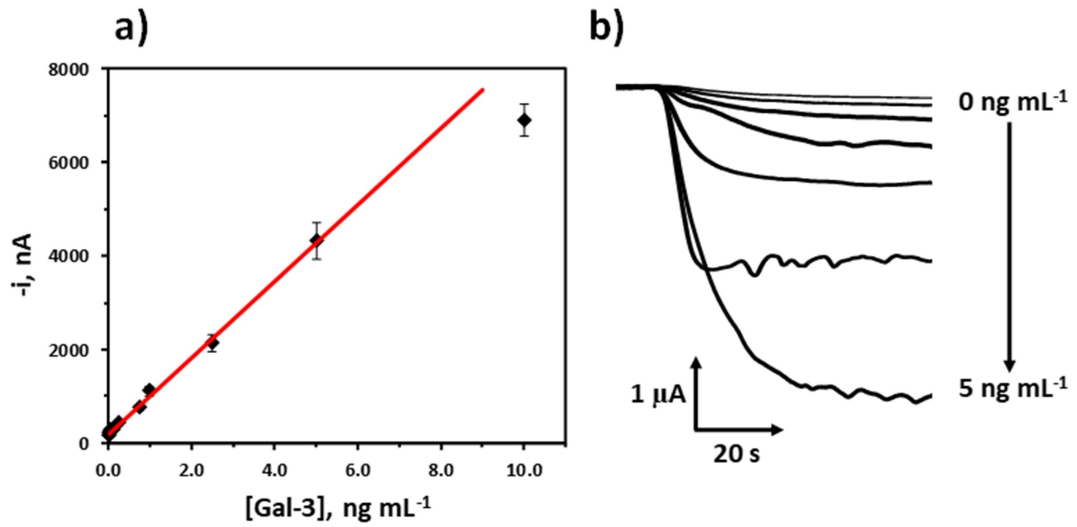

Fig. 3. Calibration curve obtained for the amperometric determination of Gal-3 standards a), and amperometric traces recorded b) by using the developed magnetic immunoplatform. Error bars estimated as triple of the standard deviation (n = 3).

surfaces has also been studied [26]. Primo et al. [25] reported a SPR method based on the use of an anti-Gal-3 antibody covalently attached to a 3-aminephenylboronic monolayer built at a thiolated Au surface modified by self-assembling of four bilayers of poly-(diallyldimethylammonium chloride) and graphene oxide. The claimed LOD value was 2 ng mL^{-1}, significantly higher than that provided by the immunosensor reported in this work.

In addition, there are several commercial ELISA methods available for Gal-3 determination claiming LODs ranging between 50 and 600 pg mL^{-1}, which are clearly higher than the obtained in this work (8.3 pg mL^{-1}). Additionally, there are several automated commercial methods such as BGM Galectin-3® test (Abbott diagnostics), Vidas®Galectin-3 (bioMérieux) or AR CHITEC Galectin-3® test (BG Medicine, Inc) that measure Gal-3 in serum or plasma within 20 min to 3 h 30 min on microtiter plate platforms, reaching LOD values ranging from 2.4 to 1.3 ng mL^{-1} [43]. Although the sensitivity of all these methods is still adequate for Gal-3 determination, they require relatively expensive instrumentation, which is hardly portable and miniaturizing.

The competitive sensitivity along with the simplicity, 1 h-assay time (once prepared the CAb-MBs) and the requirement of affordable and portable instrumentation, make the proposed MBs-based amperometric immunoplatform a proper tool, easy to automate and miniaturize, to perform Gal-3 analysis even in the outpatient routine.

3.1.3 Selectivity

The selectivity of the antibodies employed in the development of the immunosensor was assessed towards other non-target proteins (human serum albumin, HSA, hemoglobin, Hb, human immunoglobulin G, human IgG, N-terminal-pro B type natriuretic peptide, NT-proBNP, lipoprotein a, Lp(a), and soluble tyrosine kinase receptor, sAXL) present in human serum by measuring the amperometric responses for 0.0 and 1.0 ng mL^{-1} Gal-3 standards made in the absence and in the presence of the non-target proteins at the concentration levels given in the Figure 4 caption.

Figure 4 shows there were no apparent significant differences among the obtained S/B ratios in the absence and in the presence of the non-target proteins at the assayed concentration. Regardless of the S/B ratio, the amperometric signals for Gal-3 were slightly higher when HSA, hemoglobin, Lp(a) and sAXL (bars 2, 3, 6 and 7, respectively) were present in the solution, thus indicating a sort of small interference from these non-target proteins. Moreover, in the presence of hemoglobin a slightly higher signal was obtained (Figure 4, white bars 3) likely due to its intrinsic peroxidase activity [44,45]. It is worth mentioning also that the supplier of the used immunoreagents for immunosensor development claimed no potential cross-reactivity or interference towards substances with similar molecular structures such as recombinant human Gal-1, Gal-2, Gal-4 Gal-7, Gal-8 and Gal-10 (all assayed at 50 ng mL^{-1}). Noteworthy, the only electrochemical immunosensor described for Gal-3 [32] showed selectivity only against glucose, dopamine, L-threonine and BSA.

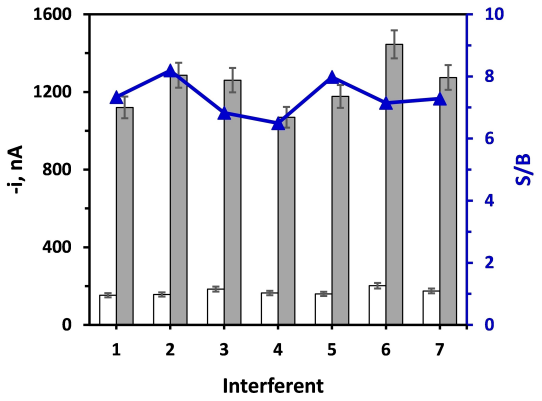

Fig. 4. Amperometric responses obtained for 0.0 (white bars) and 1.0 (grey bars) ng mL^{-1} Gal-3 standards (and the corresponding S/B ratio, blue line and triangles) prepared without (1) or with potentially interfering proteins: 0.05 mg mL^{-1} HSA (2), 0.25 mg mL^{-1} hemoglobin (3), 0.05 mg mL^{-1} human IgG (4), 0.25 ng mL^{-1} NT-proBNP (5), 1.5 μg mL^{-1} Lp(a) (6) and 3.5 ng mL^{-1} sAXL (7). Error bars estimated as triple of the standard deviation (n = 3).

3.1.4 Determination of Gal-3 in Plasma Samples from Healthy Individuals and HF Patients

The developed MBs-based immunoplatform was employed to determine Gal-3 in six plasma samples collected from healthy individuals and HF patients. The potential occurrence of matrix effect was checked by building a calibration plot using the 10-times diluted plasma samples with commercial blocker casein solution and spiked with increasing Gal-3 concentrations up to 1.0 ng mL^{-1}. The statistical comparison of the slope value of the calibration plot constructed in plasma, (1,076 ± 199) nA mL ng^{-1} and that prepared with buffered Gal-3 standard solutions, (818 ± 28) nA mL ng^{-1}, showed statistical differences ($t_{exp} = 12.4 > t_{tab} = 2.447$), thus confirming the existence of matrix effect in the diluted sample. Although dilutions larger than 10 (of 1/25 and 1/50) were tested and, as expected, gave rise to minimize the matrix effect, the amperometric signals became small provoking an unacceptable irreproducibility when they were interpolated into the calibration plot constructed with Gal-3 standards. Therefore, the Gal-3 endogenous concentration in human plasma samples was determined by using the standard additions method to the 10-times diluted samples.

The results obtained by triplicate with the immunosensor for each plasma sample (Table 2) were compared with those values obtained by using a conventional ELISA methodology involving the use of the same immunoreagents and following the protocol detailed in section 2.3. The paired samples t-test showed that no significant

Table 2. Determination of Gal-3 (ng mL^{-1}) in 10-times diluted human plasma samples with the developed MBs-based amperometric immunosensor and the conventional ELISA methodology using the same immunoreagents.

Plasma samples		MBs-based immunoassay [a]	ELISA[a]	t_{exp}
Healthy individuals	1	(4.5 ± 0.9) $RSD_{n=3}$ = 8.3 %	(4.6 ± 0.9) $RSD_{n=3}$ = 7.9 %	0.247
	2	(4.2 ± 0.3) $RSD_{n=3}$ = 3.2 %	(3.9 ± 0.6) $RSD_{n=3}$ = 8.5 %	0.605
	3	(3.4 ± 0.8) $RSD_{n=3}$ = 9.7 %	(3.6 ± 0.3) $RSD_{n=3}$ = 4.1 %	0.806
HF patients	4	(9.4 ± 0.9) $RSD_{n=3}$ = 4.3 %	(10.1 ± 0.9) $RSD_{n=3}$ = 4.5 %	1.92
	5	(11.9 ± 0.7) $RSD_{n=3}$ = 2.5 %	(11 ± 2) $RSD_{n=3}$ = 6.1 %	1.82
	6	(19 ± 2) $RSD_{n=3}$ = 4.6 %	(18 ± 3) $RSD_{n=3}$ = 8.9 %	0.682

[a] *Mean value* $\pm t \times s/\sqrt{n}$ *(n = 3; α = 0.05)*

differences were apparent for the results provided by the two methods (t_{tab} = 2.776; α = 0.05), with a correlation plot with slope and intercept values of (0.9 ± 0.1) and (46 ± 150) × 10^{-2} ng mL^{-1}, respectively.

As it can be observed, the great reproducibility and sensitivity of the developed sensor allow discriminating between healthy and HF patients, for whom in all cases Gal-3 levels higher than the lowest cut-off value set for serum, 7.57 ng mL^{-1} [40], were obtained.

3.2 Multiplexing Feasibility of the Developed Platform: Simultaneous Determination of Gal-3 and NT-proBNP

As previously mentioned, it is well-accepted that the use of a single biomarker is unlikely to be enough for a comprehensive assessment of HF diagnosis [10]. Natriuretic peptides (BNP), and N-terminal pro-brain natriuretic peptide (NT-proBNP), are well validated biomarkers in HF and recommended by current guidelines for both diagnosis and risk stratification of patients with chronic HF [5,27,46,47]. Stretching of heart muscle cells, because of cardiac volume overload, results in secretion of proBNP, which is enzymatically cleaved into BNP and NT-proBNP before being released into the bloodstream. Although both biomarkers are at the same concentration level, the circulation half-life of NT-proBNP in the body is six times longer than BNP (120 vs 20 min, respectively), making NT-proBNP a more suitable biomarker for HF [48]. However, since they are influenced by age, renal function and bodymass index, which leads to a large natural variation amongst patients [1,4,49], these natriuretic peptides have limited specificity when used individually to diagnose heart problems. In this regard, the use of strategies that combine the multiple analysis of biomarkers may be more informative and ultimately beneficial in guiding HF therapy [50]. Moreover, apart from biological processes involved in HF, Gal-3 has also revealed a role in the development of other pathological conditions such as tumorigenesis, autoimmune and inflammatory diseases [20,27,51,52].

In this context, there is substantial interest in combining Gal-3 and NT-proBNP determination to provide complementary prognostic information [5,49] and for high-risk HF patient stratification [37]. Elevated levels of Gal-3 are thought to provide independent and additive information to natriuretic peptides testing [5,10,53]. On the other hand, Gal-3 is more stable over time, has a smaller inter-individual variety, and has been shown to provide less sensitivity but higher specificity than NT-proBNP to predict CHF [9,27,54].

Several electrochemical immunosensors have been implemented for the simultaneous detection of clinical biomarkers which pair the sensitivity of electrochemistry and the specificity of antibodies with robust designs [55–58]. Nevertheless, as far as we know, there is no electrochemical immunoplatform described until now for the simultaneous determination of Gal-3 and NT-proBNP. Therefore, considering the good results obtained for Gal-3, we report here a MBs-based dual immunoplatform for the simultaneous amperometric determination of Gal-3 and NT-proBNP. The proposed platform involves the use of sandwich-type electrochemical immunosensors with B-DAbs further conjugated with Strep-HRP implemented onto MBs and coupled to disposable dSPCEs, as depicted in Figure 5a.

The possible cross-talk between the two adjacent working electrodes of the dSPCE was evaluated under the optimized conditions (see Table S1 in the supporting Information). The results are displayed in Figure 5b. No significant cross-talking was apparent due to the presence of the non-target biomarkers: blue bars in experiments (0;0) and (1;0), and orange bars in experiments (0;0) and (1;0) were not significantly different. These results confirmed the feasibility of the dual immunoplatform for the simultaneous determination of both cardiac biomarkers.

The calibration plots constructed under the optimal experimental conditions for the simultaneous determination of Gal-3 and NT-proBNP standards are displayed in Figure 5c. The linearity for Gal-3 ranges from 0.05 and 2.5 ng mL^{-1} (R^2 = 0.996), fitting the equation i (nA) = (507 ± 46) [Gal-3] (nA mL ng^{-1}) + (111 ± 48) (nA). The NT-proBNP calibration curve was linear over the 0.1–2.0 ng mL^{-1} concentration range (R^2 = 0.990) with the equation i (nA) = (467 ± 38) [NT-proBNP] (nA mL ng^{-1}) + (37 ± 36) (nA). The LOD values (calculated according to the $3 \times s_b/m$ criterion as described in *Section 3.1.2*) were 15.8 and 35.6 pg mL^{-1} for Gal-3 and NT-proBNP, respectively. The comparison of the amperometric responses measured for six different dual immunoplatforms for 1.0 ng mL^{-1} Gal-3 and 1.0 ng mL^{-1} NT-proBNP standards provided RSD values of 7.3 and 9.0 %, respectively.

The obtained analytical characteristics are still below the clinical range reported for Gal-3 in clinical samples (1.4–94.8 ng mL^{-1}) [36,37] and for NT-proBNP, whose relevant concentration range depends on age (a cut-off

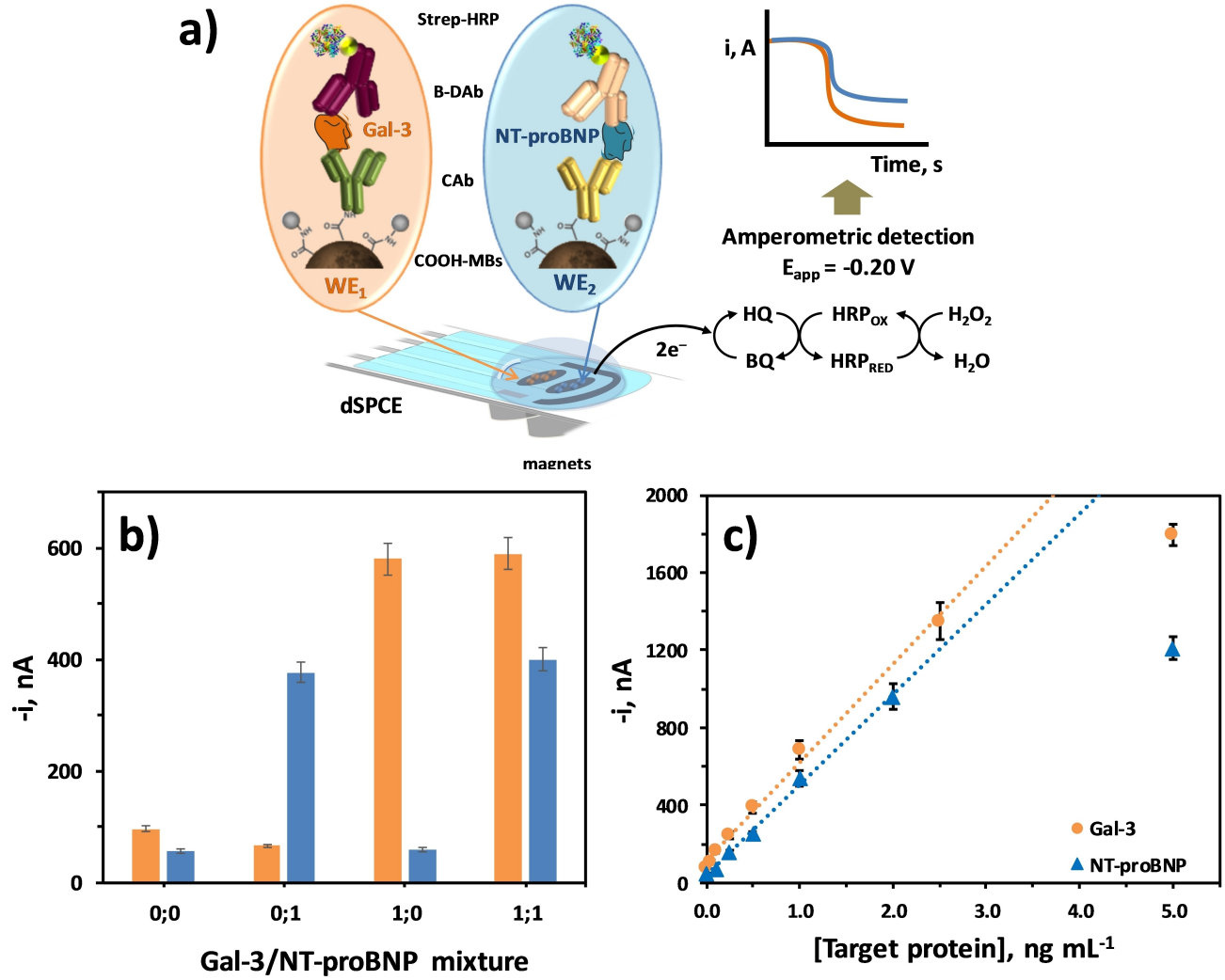

Fig. 5. Scheme and reactions involved in the MBs-based dual immunoplatform for the simultaneous determination of Gal-3 and NT-proBNP (a); Amperometric measurements performed with the dual immunoplatform (WE1: Gal-3, orange bars and WE2: NT-proBNP, blue bars) for standard mixtures containing: 0 ng mL^{-1} of both biomarkers; 1.0 ng mL^{-1} Gal-3 and 0 ng mL^{-1} NT-proBNP; 0 ng mL^{-1} Gal-3 and 1.0 ng mL^{-1} NT-proBNP; and 1.0 ng mL^{-1} Gal-3 and 1.0 ng mL^{-1} NT-proBNP (b); Calibration curves obtained for the amperometric determination of Gal-3 (orange) and NT-proBNP (blue) standards (c). Error bars estimated as triple of the standard deviation (n = 3).

value of 450 pg mL^{-1} is established for people under the age of 50, for 50–75 year old people the cut-off is 900 pg mL^{-1}, and for people older than 75 years the cut-off is 1,800 pg mL^{-1}), considering that there is no risk of HF at NT-proBNP concentrations lower than 300 pg mL^{-1} [59]. Although there are numerous methods described in the literature for the individual determination of NT-proBNP including ELISA and electrochemical biosensors [60–64], to date no electrochemical platform has been described for the simultaneous determination of NT-proBNP and Gal-3 and only one commercial ELISA kit is commercially available for the determination of these two biomarkers (from LabCorp, Test 142005) which, apart from requiring relatively expensive instrumentation (ELISA plate readers), hardly portable and miniaturizable, exhibits interference in serum samples collected from people consuming a high dose of biotin.

4 Conclusions

This work describes the first electrochemical magneto-immunoplatform developed to date for the determination of Gal-3, a biomarker of remarkable interest to diagnose and predict the progression of the cardiovascular risk. The immunoplatform is based on the formation of sandwich type immunocomplexes using biotinylated detector antibodies enzymatically labeled with Strep-HRP on MBs that are coupled to SPCEs to carry out amperometric detection by using HQ/H_2O_2. The results obtained demonstrate analytical characteristics compatible with its practical applicability providing a LOD value

1,000 times lower than the Gal-3 concentration in serum or plasma samples from healthy individuals. The developed immunoplaform proves to be competitive with other available methodologies mainly in terms of sensitivity and possibility of performing the determination at the point of care, compared to the only electrochemical immunosensor described so far in terms of simplicity and time of preparation and testing. Its potential for the determination of endogenous Gal-3 concentration in plasma samples from HF patients after a simple 1/10 dilution has been proved, providing results that agree with those attained when the same immunoreagents are used in a conventional ELISA methodology. Finally, it has also been demonstrated the possibility of exploiting this technology in the development of a dual immunosensor platform that allows simultaneous determination of Gal-3 and NT-proBNP both to consolidate the role of Gal-3 as a new biomarker for HF prognosis and to improve clinical assessment and outcomes of HF patients.

Acknowledgements

This work is part of the POSITION-II project funded by the ECSEL Joint Undertaking under grant number Ecsel-783132-Position-II-2017-IA; www.position-2.eu, and PID2019-103899RB–I00 (Ministerio de Ciencia e Innovación), and of the NANOCARDIOFLEX Project (Retos Colaboración RTC-2015-4184-1, cofinanced by the Ministerio de Economía y Competitividad and FEDER "una manera de hacer Europa"). The financial support of the RTI2018-096135-B–I00 (Ministerio de Ciencia, Innovación y Universidades) and PID2019-103899RB–I00 (Ministerio de Ciencia e Innovación) and Research Projects and the TRANSNANOAVANSENS-CM Program from the Comunidad de Madrid (Grant S2018/NMT-4349) are also gratefully acknowledged. S.V.P acknowledges the doctoral fellowship from the Fundación Carolina.

Data Availability Statement

The data that support the findings of this study are available from the corresponding authors upon reasonable request.

References

[1] T. Zhang, B. Shao, G.-A. Liu, *Eur. Rev. Med. Pharmacol. Sci.* **2017**, *21*, 4406–4410.
[2] S. L. Chow, A. S. Maisel, I. Anand, B. Bozkurt, R. A. de Boer, G. M. Felker, G. C. Fonarow, B. Greenberg, J. L. Januzzi, M. S. Kiernan, P. P. Liu, T. J. Wang, C. W. Yancy, M. R. Zile, *Circulation* **2017**, *135*, e1054–e1091. doi: 10.1161/CIR.0000000000000490.
[3] S. Paul, K. Harshaw-Ellis, *Cardiol. Rev.* **2019**, *27*, 153–159.
[4] J. Hogenhuis, A. A. Voors, T. Jaarsma, A. W. Hoes, H. L. Hillege, J. A. Kragten, D. J. van Veldhuisen, *Eur. J. Heart Failure* **2007**, *9*, 787–794.
[5] M. Felker, M. Fiuzat, L. K. Shaw, R. Clare, D. J. Whellan, L. Bettari, S. C. Shirolkar, M. Donahue, D. W. Kitzman, F. Zannad, I. L. Piña, C. M. O'Connor, G. Circ, *Heart Fail* **2012**, *5*, 2–78 doi: 0.1161/CIRCHEARTFAILURE.111.963637.
[6] C. R. de Filippi, R. H. Christenson, *JACC: Heart Failure* **2015**, *3*, 253–256.
[7] X. Yu, Y. Sun, Y. Zhao, W. Zhang, Z. Yang, Y. Gao, H. Cai, Y. Li, Q. Wang, B. Bian, J. Nie, *Int. Heart J.* **2015**, *56*, 314–318.
[8] R. A. de Boer, L. Yu, D. J. van Veldhuisen, *Curr. Heart Fail Rep.* **2010**, *7*, 1–8.
[9] N. W. van der Hoeven, M. R. Hollander, C. Yıldırım, M. F. Jansen, P. F. Teunissen, A. J. Horrevoets, T. C. T. M. van der Pouw Kraan, N. van Royen, *Vasc. Pharmacol.* **2016**, *81*, 31–41.
[10] R. R. van Kimmenade, J. L. Januzzi Jr, P. T. Ellinor, U. C. Sharma, J. A. Bakker, A. F. Low, A. Martinez, H. J. Crijns, C. A. MacRae, P. P. Menheere, Y. M. Pinto, *J. Am. Coll. Cardiol.* **2006**, *48*, 1217–1224.
[11] I. I. Eliaz, A. Patil, N. Navarro-Alvarez, Z. Wang, A. Eliaz, E. Weil, B. Wilk, D. H. Sachs, C. A. Huang, *J. Clin. Apher.* **2017**, *32*, 335–341.
[12] V. Polat, E. Bozcali, T. Uygun, S. Opan, O. Karakaya, *Acta Cardiol.* **2016**, *71*, 191–197.
[13] T. Szçke, K. Kayser, J.-D. Baumhäkel, I. Trojan, J. Furak, L. Tiszlavicz, A. Horvath, K. Szluha, H.-J. Gabius, S. Andre, *Oncology* **2005**, *69*, 167–174.
[14] C. Debray, P. Vereecken, N. Belot, P. Teillard, J. P. Brion, M. Pandolfo, R. Pocher, *Biochem. Biophys. Res. Commun.* **2004**, *325*, 1393–1398.
[15] J. Koomann, P. J. Thuluvath, M. L. Zahurak, T. Z. Kristiansen, A. Pandey, R. Schulick, P. Argani, M. Hidalgo, S. Iacobelli, M. Goggins, A. Maitra, *Cancer* **2004**, *101*, 1609–1615.
[16] V. Zivicova, P. Broz, Z. Fik, A. Mifkova, J. Plzak, Z. Cada, H. Kaltner, J. F. Kucerova, H.-J. Gabius, K. Smetana Jr, *Anticancer Res.* **2017**, *37*, 2275–2288.
[17] L. Coppin, K. Benomar, F. Corfiotti, S. Cattan, F. Renaud, C. Lapere, E. Leteurtre, M.-C. Vantyghem, S. Truant, P. Pigny, *Pancreatology* **2016**, *16*, 115–120.
[18] M. R. Raspollini, R. J. Luque, C. L. Menendez, E. Bollito, M. Brunelli, G. Martignoni, R. Montironi, L. Cheng, A. Blanca, G. Baroni, A. Minervini, A. Lopez-Beltran, *Hum. Pathol.* **2016**, *57*, 78–84.
[19] S. L. La′ulu, F. S. Apple, M. A. M. Murakami, R. Ler, W. L. Roberts, J. A. Straseski, *Clin. Biochem.* **2013**, *46*, 119–122.
[20] T. Mueller, M. Egger, I. Leitner, C. Gabriel, M. Haltmayer, B. Dieplinger, *Clin. Chim. Acta* **2016**, *456*, 19–23.
[21] M. Jovanović, J. Peter-Katalinić, *RCM* **2017**, *31*, 129–136.
[22] E. V. Moiseeva, E. M. Rapoport, N. V. Bovin, A. I. Miroshnikov, A. V. Chaadaeva, M. S. Krasilshschikova, V. K. Bojenko, C. Bijleveld, J. E. van Dijk, W. den Otter, *Breast Cancer Res. Treat.* **2005**, *91*, 227–241.
[23] A. Hittelet, H. Legendre, N. Nagy, Y. Bronckart, J.-C. Pector, I. Salmon, P. Yeaton, H.-J. Gabius, R. Kiss, I. Camby, *Int. J. Cancer* **2003**, *103*, 370–379.
[24] M. von Wolff, X. Wang, H.-J. Gabius, T. Strowitzki, *Mol. Hum. Reprod.* **2005**, *11*, 189–194.
[25] E. N. Primo, M. J. Kogan, H. E. Verdejo, S. Bollo, M. D. Rubianes, G. A. Rivas, *ACS Appl. Mater. Interfaces* **2018**, *10*, 23501–23508.
[26] K. Yoshioka, Y. Sato, T. Murakami, M. Tanaka, O. Niwa, *Anal. Chem.* **2010**, *82*, 1175–1178.
[27] D. C. Gaze, C. Prante, J. Dreier, C. Knabbe, C. Collet, J.-M. Launay, J. Franekova, A. Jabor, L. Lennartz, J. Shih, J. M. del Rey, M. Zaninotto, M. Plebani, P. O. Collinson, *Clin. Chem. Lab. Med.* **2014**, *52(6)*, 919–926.

[28] F. S. Felix, L. Angnes, *Biosens. Bioelectron.* **2018**, *10*, 470–478.
[29] E. Burcu, B. Mustafa, K. Sezgintürk, *Talanta* **2015**, *132*, 162–174.
[30] M. Pastucha, Z. Farka, K. Lacina, Z. Mikušová, P. Skládal, *Microchim. Acta* **2019**, *186*, 312. doi: 10.1007/s00604-019-3410-0.
[31] O. Y. Galkin, O. B. Besarab, M. O. Pysmenna, Y. V. Gorshunov, O. M. Dugan, *Regul. Mech. Biosyst.* **2017**, *9*, 47–55.
[32] Z. Tang, J. He, J. Chen, Y. Niu, Y. Zhao, Y. Zhang, C. Yu, *Biosens. Bioelectron.* **2018**, *101*, 253–259.
[33] M. Eguílaz, M. Moreno-Guzmán, S. Campuzano, A. González-Cortés, P. Yáñez-Sedeño, J. M. Pingarrón, *Biosens. Bioelectron.* **2010**, *26*, 517–522.
[34] C. Muñoz-San Martín, M. Gamella, M. Pedrero, A. Montero-Calle, R. Barderas, S. Campuzano, J. M. Pingarrón, *Sens. Actuators B* **2020**, *307*, 127623. doi: 10.1016/j.snb.2019.127623.
[35] C. Camacho, J. C. Matías, B. Chico, R. Cao, L. Gómez, B. K. Simpson, R. Villalonga, *Electroanalysis* **2007**, *19*, 2538–2542.
[36] N. Hrynchyshyn, P. Jourdain, M. Desnos, B. Diebold, F. Funck, *Archives of Cardiovascular Disease* **2013**, *106*, 541–546.
[37] Z. H. Amin, L. Z. Amin, I. P. Wijaya, *Clujul Med.* **2017**, *90*, 129–132.
[38] W. H. Tang, K. Shrestha, Z. Shao, A. G. Borowski, R. W. Troughton, J. D. Thomas, A. L. Klein, *Am. J. Cardiol.* **2011**, *108*, 385–390.
[39] R. A. de Boer, D. J. A. Lok, T. Jaarsma, P. van der Meer, A. A. Voors, H. L. Hillege, D. J. van Veldhuisen, *Ann. Med.* **2011**, *43*, 60–68.
[40] D. Stanojevic, S. Apostolovic, D. Stokanovic, S. Momčilović, T. Jevtovic-Stoimenov, S. Salinger-Martinovic, T. Kostic, V. N. Nikolic, *Med. Princ. Pract.* **2019**, *28*, 284–290.
[41] M. C. Martos-Maldonado, I. Quesada-Soriano, L. García Fuentes, A. Vargas-Berenguel, *Nanomaterials* **2020**, *10(2)*, 203. https://doi.org/10.3390/nano10020203.
[42] Y. K. Park, B. Bold, W. K. Lee, M. H. Jeon, K. H. An, S. Y. Jeong, Y. K. Shim, *Int. J. Mol. Sci.* **2011**, *12*, 2946–2957.
[43] W. C. Meijers, A. R. van der Velde, R. A. de Boer, *Expert Rev. Mol. Diagn.* **2014**, *14*, 257–266.
[44] D. V. Grigorieva, I. V. Gorudko, A. V. Sokolov, O. V. Kosmachevskaya, A. F. Topunov, I. V. Buko, E. E. Konstantinova, S. N. Cherenkevich, O. M. Panasenk, *Bull. Exp. Biol. Med.* **2013**, *155*, 118–121.
[45] A. Kapralov, I. I. Vlasova, W. Feng, A. Maeda, K. Walson, V. A. Tyurin, Z. Huang, R. K. Aneja, J. Carcillo, H. Bayır, V. E. Kagan, *J. Biol. Chem.* **2009**, *284*, 30395–30407.
[46] J. A. Doust, E. Pietrzak, A. Dobson, P. Glasziou, *BMJ* **2005**, *330*, 625. doi: 10.1136/bmj.330.7492.625.
[47] C. W. Yancy, M. Jessup, B. Bozkurt, J. Butler, D. E. Casey Jr, M. M. Colvin, M. H. Drazner, G. S. Filippatos, G. C. Fonarow, M. M. Givertz, S. M. Hollenberg, J. Lindenfeld, F. A. Masoudi, P. E. McBride, P. N. Peterson, L. W. Stevenson, C. Westlake, *JACC* **2017**, *70*, 776–803.
[48] H.-N. Kim, J. L. Januzzi, *Circulation* **2011**, *123*, 2015–2019.
[49] D. J. A. Lok, P. Van Der Meer, P. W. Bruggink-André de la Porte, E. Lipsic, J. Van Wijngaarden, H. L. Hillege, D. J. van Veldhuisen, *Clin. Res. Cardiol.* **2010**, *99*, 323–328.
[50] J. Lassus, E. Gayat, C. Mueller, V.-P. Harjola, R. van Kimmenade, A. Pathak, T. Mueller, S. Disomma, M. Metra, D. Pascual-Figal, S. Laribi, S. Logeart, N. Nouira, M. Sato, J. Potocki, C. Parenica, A. Collet, J. L. Cohen-Solal, D. Januzzi Jr, A. Mebaza, *Int. J. Cardiol.* **2013**, *168*, 2186–2194.
[51] R. H. Christenson, S. H. Duh, A. H. Wu, et al, *Clin. Biochem.* **2010**, *43*, 683–690.
[52] R. Dong, M. Zhang, Q. Hu, S. Zheng, A. Soh, Y. Zheng, H. Yuan, *Int. J. Mol. Med.* **2018**, *41*, 599–614.
[53] B. Zethelius, L. Berglund, J. Sundström, E. Ingelsson, S. Basu, A. Larsson, P. Venge, J. Ärnlöv, *N. Engl. J. Med.* **2008**, *358*, 2107–2116.
[54] K. Chen, R. J. Jiang, C. Q. Wang, Z. F. Yin, Y. Q. Fan, J. T. Cao, Z.-H. Han, Y. Wang, D.-Q. Song, *Eur. Rev. Med. Pharmacol. Sci.* **2013**, *17*, 1005–1011.
[55] B. Esteban-Fernández de Ávila, V. Escamilla-Gómez, V. Lanzone, S. Campuzano, M. Pedrero, D. Compagnone, J. M. Pingarrón, *Electroanalysis* **2014**, *26*, 254–261.
[56] F. Zhou, M. Lu, W. Wang, Z.-P. Bian, J.-R. Zhang, J.-J. Zhu, *Clin. Chem.* **2010**, *56*, 1701–1707.
[57] J. Wu, J. Yan, F. Yan, H. Ju, *Anal. Chem.* **2008**, *80*, 6072–6077.
[58] R. Polsky, J. C. Harper, D. R. Wheeler, S. M. Dirk, D. C. Arango, S. M. Brozik, *Biosens. Bioelectron.* **2008**, *23*, 757–764.
[59] E. Roberts, A. J. Ludman, K. Dworzynski, A. Al-Mohammad, M. R. Cowie, J. J. V. McMurray, J. Mant, *BMJ* **2015**, *350*, h910. doi: 10.1136/bmj.h910.
[60] Y. Zhuo, W. J. Yi, W. B. Lian, R. Yuan, Y. Q. Cha, A. Chen, C. H. Hu, *Biosens. Bioelectron.* **2011**, *26*, 2188–2193.
[61] W. Yi, W. Liang, P. Li, S. Li, Z. Zhang, M. Yang, A. Chen, B. Zhang, C. Hu, *Biotechnol. Lett.* **2011**, *33*, 1539–1543.
[62] W. Liang, Y. Li, B. Zhang, Z. Zhang, A. Chen, D. Qi, W. Yi, C. Hu, *Biosens. Bioelectron.* **2012**, *31*, 480–485.
[63] B. Esteban-Fernández de Ávila, V. Escamilla-Gómez, S. Campuzano, M. Pedrero, J. M. Pingarrón, *Anal. Chim. Acta* **2013**, *784*, 18–24.
[64] W. M. Munief, X. Lu, T. Teucke, J. Wilhelm, A. Britz, F. Hempel, R. Lanche, M. Schwartz, J. Ka Yan Law, S. Grandthyll, F. Müller, J. V. Neurohr, K. Jacobs, M. Schmitt, V. Pachauri, R. Hempelmann, S. Ingebrandt, *Biosens. Bioelectron.* **2019**, *126*, 136–142.

Received: July 9, 2020
Accepted: August 17, 2020
Published online on September 3, 2020

